In these formulas p should be substituted according to formula (4) and the form of the function $f_T(m, n, s)$ is according to formula (1).

For the first scenario, which is characterized by the lack of correlation between $\boldsymbol{R}_b$ and $\boldsymbol{R}_t$, calculations of each probability were done using the fact that the probability q of a miss in a single shot is given by formula (11) when one substitutes $N = 1$. Then the probability of hit with a single shot equals

$$p = 1 - q \tag{15}$$

and the other values of probabilities are defined by the formulas of the same structure as the formulas (5–9).

Probability of Killing by the Fragments of the Shell, Taking into Account the Motion of the Target

The presented probability models allow the fragmentation action of a round equipped with a proximity, time, or programmed fuse to be taken into account. It has to be noted that there is a difference between firing a round equipped with proximity fuse and a round with time or programmed fuse. In the first case one can assume that the random vector process describing the location of the round's blast epicenter in relation to the target is equal to $\boldsymbol{R}_t$ or $\boldsymbol{R}_t'$. In the second case the discussed random vector process is a function of $\boldsymbol{R}_t$ or $\boldsymbol{R}_t'$ and a random variable T describing the time from the moment the round leaves the barrel to the moment of blast. This variable takes into account the systematic error that originates in the dispersion of delayed burning time or the dispersion of a timer-counting mechanism.

In both cases of the presented models one should then substitute the conditional killing probability P_r by the DF $P_r(x_1, x_2, x_3)$. The form of formulas describing the probabilities P_R, P_{R1}, P_E, and P_{E1} would depend on the form of the DF, and consequently, each case should be analyzed individually.

Example Numerical Results

The calculations were made for an extreme case when a target of 8 m length by 2 m height moves at a distance of 3000 m, just above the ground level in a direction perpendicular to the axis of the barrel, with the velocity of 250 or 50 m/s. The AA battery consists of a twin 30 mm × 170 Mauser cannon ($N = 70$, $P_r = 0.37$) or a twin 35 mm × 228 Oerlikon cannon ($N = 35$, $P_r = 0.5$). The values of N and P_r were set according to Refs. 3 and 6. It was additionally assumed that for both calibers $\boldsymbol{R}_b$ and $\boldsymbol{R}_t$ are the same and the respective standard deviations equal: $\sigma_{t1} = \sigma_{t2} = 1.8$ m; $\sigma_{t3} = 2.0$ m; $\sigma_1 = \sigma_2 = 4.5$ m, $\sigma_3 = 9.0$ m. The results are given in Tables 1 and 2.

Table 1 Values of probability when there is correlation between $\boldsymbol{R}_b$ and $\boldsymbol{R}_t$

Probabilities	30 mm × 170 v_c = 250 m/s	35 mm × 228 v_c = 250 m/s	35 mm × 228 v_c = 50 m/s
P_R	0.3666	0.4688	0.4846
P_M	0.0091	0.0624	0.0309
P_E	0.6243	0.4688	0.4846

Table 2 Values of probability when there is no correlation between $\boldsymbol{R}_b$ and $\boldsymbol{R}_t$

Probabilities	30 mm × 170 v_c = 250 m/s	35 mm × 228 v_c = 250 m/s	35 mm × 228 v_c = 50 m/s
P_R	0.8314	0.7514	0.8279
P_M	0.0073	0.0584	0.0271
P_E	0.1613	0.1902	0.1415

Conclusions

The numerical results presented indicate the strong influence of the method of laying the gun on the final probability value. Correcting the aiming for each shot in a burst approximately doubles the probability P_R. However, it does not affect significantly the value of the probability P_M. It also has to be noted that there is relatively weak influence of the target velocity on the values of probability.

References

[1]Przemieniecki, J. S., *Introduction to Mathematical Methods in Defense Analyses*, AIAA Education Series, AIAA, Washington, DC, 1990.

[2]Anon., "Effect of Proximity-Fuzed Air Defense Ammunition," Information Document of Bofors AB, Bofors, Sweden, 1992.

[3]Orlov, B. W. (ed.), *Proektirovanie raketnyh i stvolnyh sistem*, Mashinostroenie, Moscow, 1974.

[4]Brändli, H., *Waffe und Wirkung bei der Fliegerabwehr*, Birghauserverlag, Basel, Switzerland, 1956.

[5]Garner, F., "Hit Probability for Small and Medium Calibre Belt-Fed Cannon," *International Defense Review*, Vol. 11, 1991, pp. 1244–1249.

[6]Germershausen, R. (ed.), *Waffentechnisches Taschenbuch*, Rheinmetall, Düsseldorf, Germany, 1980.

[7]Pogorzelski, W., "Badania nad zagadnieniem prawdopodobieństwa trafienia w teorii strzelania do samolotu," *Wiadomosci Techniczne Uzbrojenia*, Vol. 44, Warsaw, Poland, 1939, pp. 205–231.

[8]Papoulis, A., *Probability, Random Variables, and Stochastic Processes*, McGraw-Hill, New York, 1965.

Simulation of DD-963 Ship Airwake by Navier–Stokes Method

Tsze C. Tai*
U.S. Naval Surface Warfare Center, Bethesda, Maryland 20084
and
Dean Carico†
U.S. Naval Air Warfare Center, Patuxent River, Maryland 20670

Introduction

THE ship airwake is defined as an arbitrary volume of air, namely an air burble, surrounding the ship. The effect of airwake on aircraft/ship interface operation is determined by the airflow disturbances caused by the ship that are perceptible to the pilot during the final approach and landing in a shipboard operation. A better understanding of the airwake effect would improve aircraft operations in a seabase interface environment.[1,2]

The complexity of the ship airwake problem requires the use of a Navier–Stokes-type method to reveal correct flow features. Advances in numerical algorithm schemes along with increased computer speed and capacity have made it feasible

Presented as Paper 93-3002 at the AIAA 24th Fluid Dynamics Conference, Orlando, FL, July 6–9, 1993; received Sept. 12, 1993; revision received April 13, 1995; accepted for publication May 15, 1995.

*Senior Research Scientist, Carderock Division, Sea Based Aviation Office. Associate Fellow AIAA.

†Rotorcraft Simulation Specialist, Aircraft Division, Rotary Wing Aircraft Test Directorate. Member AIAA.

to provide answers to complex aerodynamic problems in computational fluid dynamics (CFD). Although physical modeling of unsteady, vortex-dominated flows over complex geometry remains prohibitive, reasonably accurate simulated results based on steady-state solutions have been obtained during the past decade. This Note describes simulating the airwake of a DD-963 ship configuration by using a multizone, thin-layer Navier–Stokes method.

Computational Method

Three-dimensional codes based on Reynolds stress-averaged Navier–Stokes equations for steady or unsteady flows have been developed in the past decade. In particular, the thin-layer codes are cost effective and adequate for application to many aerodynamic problems with complex geometry. The CFL3D code[3] of NASA Langley is used as the flow solver. The code is based on the thin-layer approximation of the Reynolds stress-averaged Navier–Stokes equations. A finite volume algorithm with a spatially factored diagonalized, implicit scheme is used in discretization of the partial differential equations. The upwind-biased-differencing using the flux-difference-splitting technique is employed. A variety of turbulence models are available; their accuracy and adequacy were discussed by Rumsey.[4] In the present work, the Baldwin–Lomax model along with the Degani–Schiff modification for proper length scales for separated flow is used. The code is capable of multizone flow solving through a grid-patching scheme.

A structured, curvilinear, body-conforming grid is generated. The front and midisland superstructures of the DD-963 ship are represented by two numerical blocked structures, followed by a flight deck, and a lower missile deck. The computational model, which is a compromise between the real ship configuration and a previous wind-tunnel model, consists of a series of rectangular volume blocks in tandem (see Fig. 1). The NASA Ames 3DGRAPE code[5] is used for basic grid generations. A cylindrical grid topology is adopted for its capability to treat a body with a sharp nose. The topology is basically an H-O mixed type, with H-type in the longitudinal plane, and O-type in the crossflow plane. The outer cylindrical surface is set at 2.5 ship lengths from the ship centerline. The most forward plane is set at 1.0 ship length from the bow of the ship and 3.0 ship lengths from the stern. Assuming symmetry about the centerplane, only the right half of the ship needs to be modeled. This size has been employed in other configurations and proved to be adequate. The topology allows a simplified DD-963 ship configuration to be modeled and combined into one single grid.

The boundary conditions for the Navier–Stokes flow solver are 1) atmospheric boundary-layer flow at upstream, 2) atmospheric pressure recovery at downstream, 3) characteristic form of inflow–outflow at the cylindrical outer boundary, and 4) viscous nonslip flow at the surface of the ship. The atmospheric boundary layer is approximated by a power-law profile with a power of 0.12. The water surface is assumed to be flat and waveless, and the flow properties in the airwake remain unmixed with the water. The assumption makes the water surface neither viscous nor inviscid. Thus, a reflective boundary is applied. The application in fact is a postpriori after some other attempts of treating the water boundary failed. It turns out to be a fairly good approximation after all, except that the vertical velocity component must vanish at the water surface.

Results and Discussion

Airwake data were obtained for a DD-963 ship configuration subject to an atmospheric wind speed of 10 kn (Mach 0.015) and 30 kn (Mach 0.045), both at 30 deg with respect to the ship bow. The flow condition yields a Reynolds number range of 1.77×10^8 based on the ship length for the full-size ship, and 7.1×10^4 based on beam length of a 1/140-scale model. If the ship's beam is used for the Reynolds number basis, the high figure would have to be reduced approximately by a factor of 10. The higher end of the spectrum of Reynolds numbers falls into the turbulent flow range, whereas the lower end results in a laminar flow. Both low and high Reynolds numbers are considered. The low Reynolds number case is taken for the purpose of comparison with available wind-tunnel data. Converged results were obtained in about 6,000 to 7,000 iterations (time steps) requiring approximately 7–8 h of Cray Y-MP CPU time.

Figure 2 shows the computed particle trace of the streamlines emanating from various stations on the ship surface at a Reynolds number of 7.1×10^4. The flow is mostly separated, with free vortices originating from virtually all sections. There are two types of separation: one due to viscosity and the other due to sharp corners of the blocked structures. They are marked in the figure. The former is closely influenced by the types of flow involved that can be distinguished by the Reynolds number. The latter is purely an inviscid phenomenon, independent of Reynolds number. The size of air burble (airwake) is greatly influenced by both of them. In addition to free vortices, massive separated flow regions are found behind the structures, including the flight deck.

In Fig. 3, which is another view (rear view) of the same particle trace, the flow pattern over the flight deck is compared with a sketch based on wind-tunnel measurements (Fig. 5 of Ref. 6). The flow, very complex in nature, results from both the viscous/vortex and vortex/inertial interactions. Most physical flow features are well captured by the simulated results. Figure 4 depicts the contour of the longitudinal velocity components at the ship's center plane. The numerical numbers imply values of velocity components normalized by the

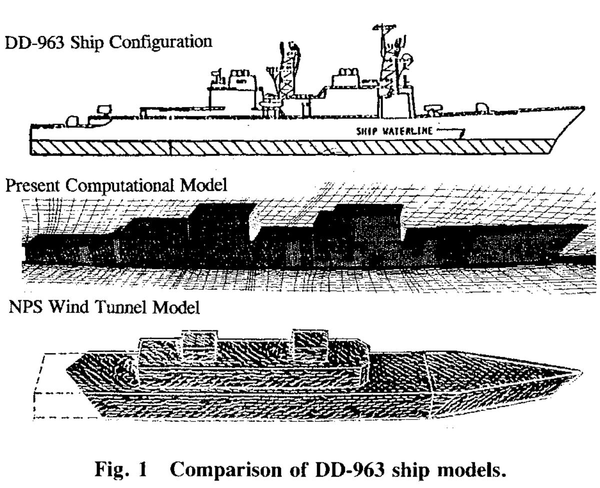

Fig. 1 Comparison of DD-963 ship models.

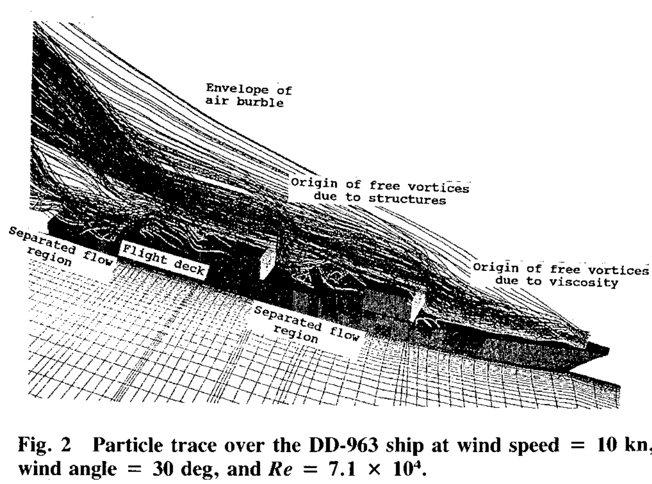

Fig. 2 Particle trace over the DD-963 ship at wind speed = 10 kn, wind angle = 30 deg, and $Re = 7.1 \times 10^4$.

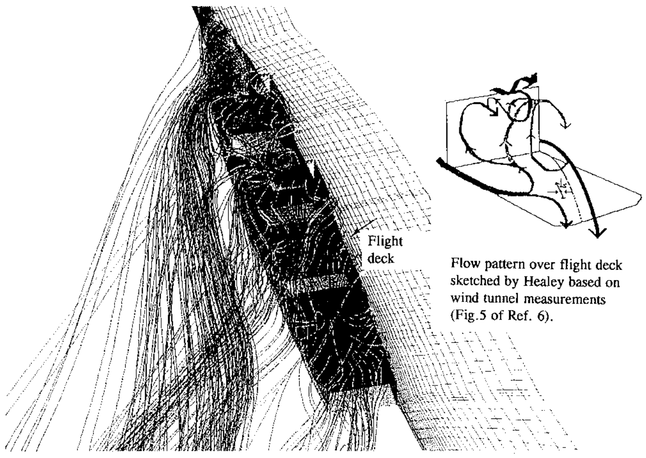

Fig. 3 Flow pattern over the flight deck.

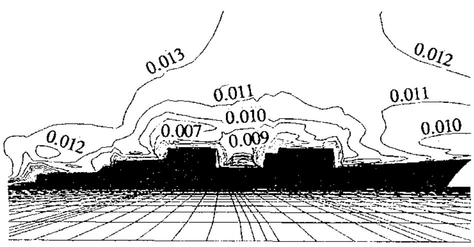

Fig. 4 Contour of longitudinal velocity along center plane, wind speed = 10 kn, wind angle = 30 deg, and Re = 7.1 × 10[4].

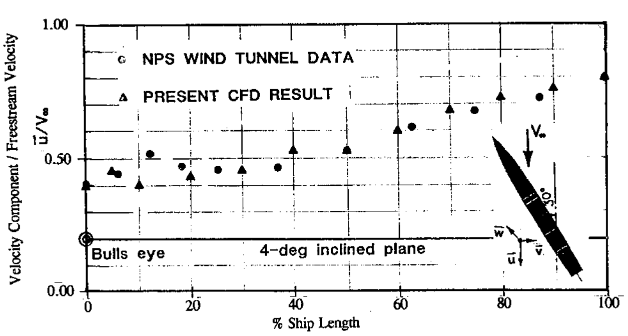

Fig. 5 Comparison of simulated results with wind-tunnel measurements, wind speed = 10 kn and wind angle = 30 deg.

speed of sound. The velocities contain large deficiencies in the regions involving massive flow separation.

Comparison of the present results with the wind-tunnel data measured previously at the Naval Postgraduate School[6,7] is given in Fig. 5. The data are distributed along a path that measures from the bulls-eye to one ship length away along a 4-deg inclined plane. A striking agreement is observed, except in the near field where the formation of vortical flow structures takes place. The measurement at the bulls-eye was taken at a height z/L = 0.017 (L is ship length).

A wind-over-the-deck of a 30-kn wind at an angle of 30 deg is used to investigate the effect of wind speed. The Reynolds number is proportionally increased to 21.3×10^4 for the scaled model and 1.77×10^8 for a full-size ship. These numbers qualify the flow to be in the laminar and turbulent flow ranges, respectively. Figure 6 shows the particle trace over the ship subject to 30-kn atmospheric wind at a wind angle of 30 deg and a Reynolds number of 1.77×10^8. The flow pattern, in general, resembles the 10-kn wind case, except that there appear more free-vortex spirals in the leeside of the ship. Because of its very high Reynolds number, the flow exhibits characteristics of fully developed turbulent shear layers. As a result, the size of the airwake is reduced accordingly, and the free vortex spirals that originated in the front and rear sections of the ship become more apparent.

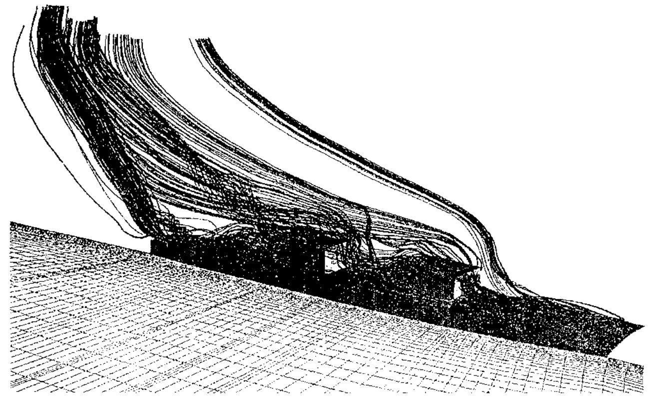

Fig. 6 Particle trace over DD-963 ship at wind speed = 30 kn, wind angle = 30 deg, and Re = 1.77 × 10[8].

Concluding Remarks

The airwake of a DD-963 ship configuration subject to atmospheric winds of 10 and 30 kn at a wind angle of 30 deg is simulated by using a multizone, thin-layer Navier–Stokes method. Both laminar and turbulent flow conditions were considered. The resulting flow contains regions of massive flow separation along with free vortices. Major flow features including viscous–vortex interactions observed in wind-tunnel experiments are captured. The computed streamwise velocities along a specified flight path compare well with wind-tunnel data. For a given wind speed, the high Reynolds number condition that corresponds to the full-scale ship, has a tendency of reducing the overall size of airwake. On the other hand, there is only a small difference in flow pattern for different wind speeds considered.

Full-scale DD-963 ship airwake measurements, covering significant range of wind-over-the-deck speed and direction, are needed for validations. Future research should consider the sensitivity of the level of detail in the computational ship model, as well as different ship pitch and roll trim angles.

Acknowledgments

The present work was supported by the Naval Air Systems Command. NASA Ames Research Center provided the Cray CPU time.

References

[1]Healey, J. V., "The Prospects for Simulating the Helicopter/Ship Interface," *Naval Engineer Journal*, Vol. 99, No. 2, 1987, pp. 45–63.

[2]Carico, D., Reddy, W., and DiMarzio, C., "Ship Airwake Measurement and Modeling Options for Rotorcraft Applications," AGARD Symposium on Aircraft Ship Operations, Paper 100, Seville, Spain, May 1991.

[3]Thomas, J. L., Walters, R. W., Reu, T., Ghaffari, F., Weston, R. P., and Luckring, J. M., "Application of a Patched-Grid Algorithm to the F/A-18 Forebody-Leading-Edge Extension Configuration," *Journal of Aircraft*, Vol. 27, No. 9, 1990, pp. 749–756.

[4]Rumsey, C. L., and Vatsa, V. N., "A Comparison of the Predictive Capabilities of Several Turbulence Models Using Upwind and Central-Difference Computer Codes," AIAA Paper 93-0192, Jan. 1993.

[5]Sorenson, R. L., "The 3DGRAPE Book: Theory, Users' Manual, Examples," NASA TM 102224, July 1989.

[6]Healey, J. V., "The Airwake of a DD-963 Class Destroyer," *Naval Engineer Journal*, Vol. 101, No. 2, 1989, pp. 36–42.

[7]Healey, J. V., "A Data Base for Flight in the Wake of a Ship," AIAA Paper 92-0295, Jan. 1992.